

**Annual Report, 1999**  
**Response of the Ventura basin to the Northridge Earthquake**

**Principal Investigator: Andrea Donnellan**  
**Co-Investigators: Gregory A. Lyzenga and Jay W. Parker**

**Jet Propulsion Laboratory**

Results from campaign data and continuous SCIGN data indicate that a narrow band of shortening runs along the front of the Transverse Ranges through the Ventura and northern Los Angeles basins (Donnellan et al, 1993; Argus et al, 1999). The shortening rates are 7-10 mm/yr and 5-6 mm/yr for the Ventura and Los Angeles basins. Analysis of the data shows nearly pure shortening indicating thrust faulting environments.

Forward and inverse elastic modeling, when combined with geologic data, proved useful in estimating fault slip rate and geometry for the Ventura basin. The Northridge earthquake occurred along the southeastern portion of the basin on a fault similar to that defined by elastic forward models. The models required that the faults bounding the basin be creeping from the lower crust up to within about 5 km of the surface. The Northridge earthquake ruptured from a depth of 18 km. This leads to a problem. Can faults both creep and be seismogenic or are they completely locked to their seismogenic depth?

Viscoelastic finite element models in which a ductile lower crust relaxes between earthquakes and the basin is of compliant sediments explains the concentrated strain rates and deep seismogenic depths (Hager et al, 1999). The models are useful in bounding the long-term shortening rate across the basin, because there is a trade-off between shortening rate and lower crustal viscosity. Based on the geology a longer relaxation time (stiffer lower crust) and lower geological rate is favored.

The observable postseismic transients decay with time with most of the motion occurring within the first year after the earthquake. The horizontal and vertical postseismic motions, at stations where they are significant, can be fit fairly well by an exponential time dependence, with a characteristic decay time in the range 0.3-1.4 years. Both the horizontal and vertical motions can be fit equally well (or perhaps slightly better) by a logarithmic function (Marone et al., 1991). Exponential decay characterizes relaxation of a Maxwell viscoelastic solid, while fault afterslip may be expected to obey a logarithmic

law. These results imply that we are unable to distinguish between afterslip and relaxation mechanisms. The models presented here suggest that both processes may have occurred following the earthquake.

The best model that allows for slip on one plane prefers the slip to be located above the upper portion of the rupture zone. The data do not permit slip on the downdip extension. If we restrict the slip such that it occurs only on the downdip extension of the fault, the misfit of the residuals ( $\chi^2/\text{dof}$ ) is large ( $\sim 5$ ). If we free up various parameters, the slip is either located above 18 km, or the fit is unrealistic (e.g., extremely large slip on an extremely narrow fault). Similar results occur for slip on the updip extension of the fault; the afterslip does not extend updip from the rupture plane.

In a second set of inversions, we solved for an auxiliary fault while fixing and freeing various parameters. This heuristic approach was dictated by the limited degrees of freedom and data strength afforded by the sparse data set. In each of these inversions nearly pure thrust afterslip occurs on one fault that fits the entire mainshock rupture plane. No slip extends above or below the rupture plane, and with the addition of a second fault the slip does not extend beyond the rupture plane laterally. We present the best model here; however, it should be taken as broadly representative of the possible postseismic mechanisms. We experimented with dozens of models by varying the initial values and fixed parameters. Afterslip on the main fault and additional slip on an auxiliary fault emerge as the best fitting models. The auxiliary fault does not correspond to any mapped fault but may rather be indicative of general deformation of the upper crust as a result of the mainshock. This "fault," which is more likely representative of broad deformation in the upper crust, coincides with shallow aftershocks that are also interpreted as deformation of a quasi-elastic material.

InSAR observations were employed to obtain additional constraint on the postseismic deformation source. An interferogram was produced from ERS-1 SAR data for frames obtained for November of 1993 and December of 1995. The time period is close to the time period of the GPS data. The SAR data correlated well in the San Fernando Valley where much of the deformation from the Northridge earthquake took place. Decorrelation occurred in the hills to the north of the valley.

The interferogram of Figure 1 shows a combination of the coseismic and postseismic crustal deformation signal. We subtracted a synthetically generated interferogram of the model of Wald and Heaton (1996) to produce an image of the postseismic deformation. shown in Figure 2 is a synthetic interferogram using the GPS inversion for postseismic creep described above. We scaled the magnitude of the observations according to the

logarithmic fit to the data. The inversion and postseismic SAR observations are qualitatively similar. We see deformation over the rupture plane and to the west of the rupture. The magnitude of the deformation is similar in both cases.

Additional models of this deformation mechanism are in development. We are currently using two classes of models to support our data interpretation effort. We have developed a set of forward and inversion codes based on Okada's methods (1985). These are isotropic elastic models for which 9 fault parameters can be solved (location, depth, dip, length, width, slip). The inversion model uses a residual-minimization procedure based on a downhill simplex simulated annealing algorithm (Lyzenga et al., 1999).

We are also expanding two-dimensional finite element code to three dimensions. The code includes a sophisticated mesh generator to simplify the complex gridding process. The mesh generator generates a mesh based on specified geometry and rheologies and densifies the mesh where necessary. The code includes viscoelastic linear or nonlinear rheology, and split nodes.

Ongoing development of the finite element code and associated utilities is aimed at a pair of complementary scientific goals. The addition of mature three-dimensional modeling tools will begin to enable, for the first time, realistic simulations of real-world configurations of multiple faults and non-planar fault configurations. This ability will be essential for detailed understanding of complex tectonic environments like the Los Angeles and Ventura basin regions. Secondly, these advanced tools will enable the development of a new level of theoretical intuition and understanding of the evolution and behavior of complex systems of faults and deforming continua. The relative roles of rheology, 3-d geometry, fault mechanics and boundary conditions will become much better understood through the study of these models.

## **References**

Argus and Heflin, 1995, Plate motion and crustal deformation associated with geodetic data from the Global Positioning System, *Geophys. Res. Lett.*, 22, 1973-1976.

Argus, D. F., M. B. Heflin, A. Donnellan, F. H. Webb, D. Dong, K. J. Hurst, D. C. Jefferson, G. A. Lyzenga, M. M. Watkins, J. F. Zumberge, Shortening and Thickening of Metropolitan Los Angeles Measured and Inferred Using Geodesy, *Geology.*, 27, 703-706 (1999).

Donnellan et al., 1993, Discrepancy between geologic and geodetic deformation rates in the Ventura basin, *Nature*, 366, 333-336.

Donnellan and Lyzenga, 1998, GPS Observations of fault afterslip and upper crustal deformation following the Northridge earthquake, *J. Geophys. Res.*, 103, 21,285-21,297.

Hager, B. H., G. A. Lyzenga, A. Donnellan, D. Dong, Reconciling Rapid Strain Accumulation with Deep Seismogenic Fault Planes in the Ventura Basin, California, *J. Geophys. Res.*, 104, 25,207-25,219 (1999).

Lyzenga, G. A., W. R. Panero and A. Donnellan, The Influence of Anelastic Surface Layers on Postseismic Thrust Fault Deformation, *J. Geophys. Res.*, in press (2000).

Okada, 1985, Surface deformation due to shear and tensile faults in a half-space, *Bull. Seism. Soc. Am.*, 75, 1135-1154.

Peltzer et al, manuscript in preparation, InSAR observations of the Northridge Earthquake.

Shen et al., 1996, Crustal deformation across and beyond the Los Angeles basin from geodetic measurements.

Zumberge et al., 1997, Precise point positioning for the efficient and robust analysis of GPS data from large networks, *J. Geophys. Res.*, 102, 5005-5017.

.

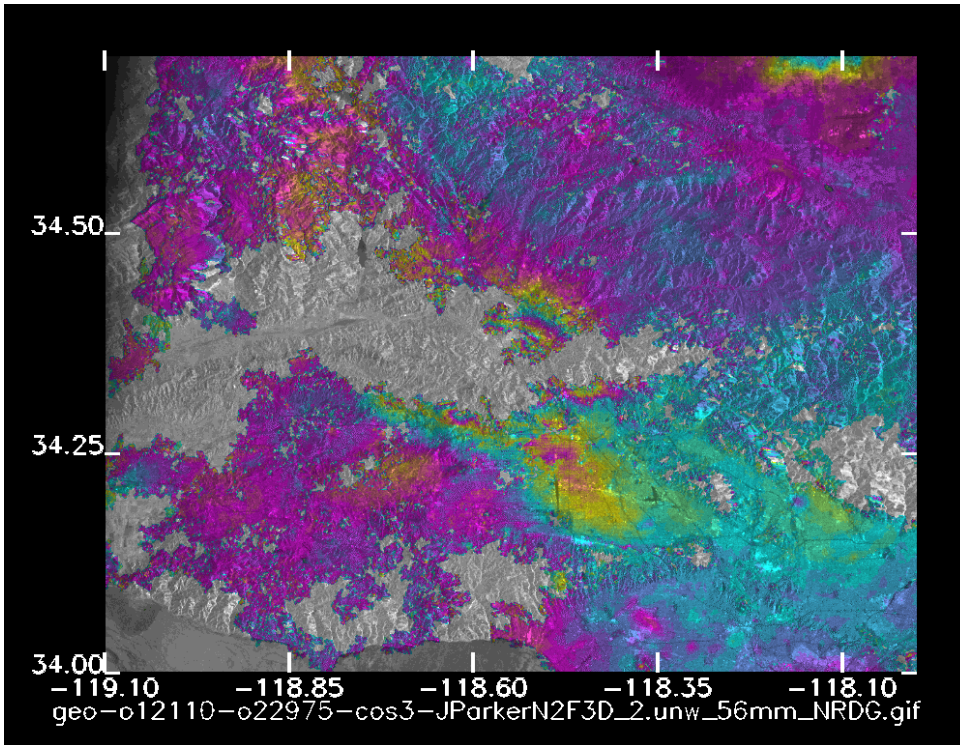


Figure 1

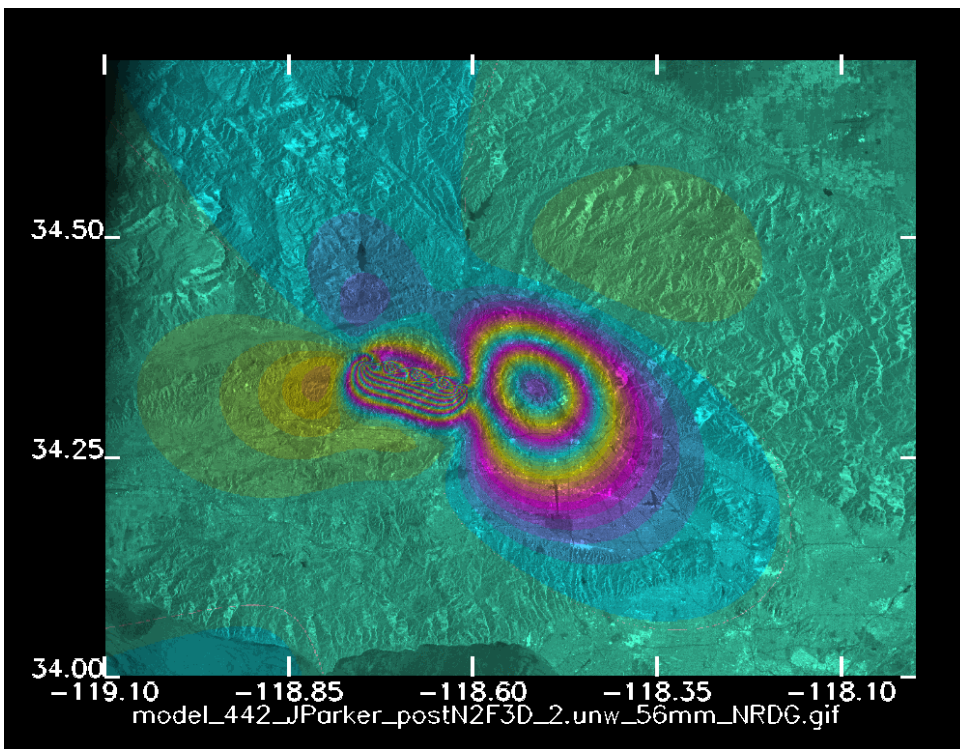


Figure2